Spatially resolved series resistance of silicon solar cells obtained from luminescence imaging

T. Trupke,[a] E. Pink, R. A. Bardos, and M. D. Abbott
Centre of Excellence for Advanced Silicon Photovoltaics and Photonics, University of New South Wales, Sydney 2052, Australia

(Received 7 January 2007; accepted 23 January 2007; published online 28 February 2007)

The fast determination of the spatially resolved series resistance of silicon solar cells from luminescence images is demonstrated. Strong lateral variation of the series resistance determined from luminescence images taken on an industrial screen printed silicon solar cell is confirmed qualitatively by a Corescan measurement and quantitatively by comparison with the total series resistance obtained from the terminal characteristics of the cell. Compared to existing techniques that measure the spatially resolved series resistance, luminescence imaging has the advantage that it is nondestructive and orders of magnitude faster. © *2007 American Institute of Physics*.
[DOI: 10.1063/1.2709630]

The series resistance of silicon solar cells often exhibits strong lateral variations, particularly in industrial screen printed cells. Experimental techniques to quantify such variations include Corescan,[1] Cello,[2] and imaging techniques based on dark and illuminated infrared lock-in thermography (LIT).[3,4] These techniques require data acquisition times between minutes and several hours per solar cell. Electroluminescence (EL) and photoluminescence (PL) imaging are very fast characterization tools for silicon solar cells and silicon wafers, with data acquisition times of a few seconds or less per sample.[5,6] Using EL images and PL images taken with external control of the voltage to measure lateral variations of the series resistance in silicon solar cells was proposed in Ref. 7. Some preliminary qualitative results were also reported.[7,8] Here, we demonstrate a *quantitative* determination of the series resistance and its lateral variation in a monocrystalline industrial screen printed silicon solar cell by luminescence imaging.

Photoluminescence images are taken using an 815 nm/25 W laser that is expanded to illuminate the cell area of 12.5×12.5 cm^2 homogeneously with up to 0.67 Sun equivalent illumination intensity. A thermoelectrically cooled silicon charge coupled device camera is used to capture luminescence images. For the PL images with simultaneous current extraction, two arrays of ten spring loaded contact pins are used to contact the busbars of the cell homogeneously. A commercially available instrument is used for Corescan measurements; illuminated *IV* curves are measured with a calibrated industrial cell tester.

In a simplified case, a solar cell is described as a two-dimensional network of parallel nodes, with each node consisting of a series connection of a local resistor $R_{s,i}$ and a diode. The value of $R_{s,i}$ is given as

$$R_{s,i}=\frac{\Delta U_{R_{s,i}}}{I_i}, \tag{1}$$

where $\Delta U_{R_{s,i}}$ is the local voltage drop over the series resistance and I_i the local current, which is calculated from the local current density J_i and the area of each node (i.e., each pixel). Our approach to measure $R_{s,i}$ is to determine $\Delta U_{R_{s,i}}$ from luminescence images while operating the cell under conditions at which reasonably accurate assumptions can be made about J_i.

Using luminescence intensities as an indicator of the diode voltage has previously been demonstrated.[9,10] However, under illumination and at low terminal voltages the carrier density within the bulk is diffusion limited, which leads to an error in the predicted so-called *implied voltage*. Under such operating conditions we therefore propose to use the total carrier concentration at a given operating point minus the total carrier concentration measured with the same illumination intensity but at short circuit as an indicator for the diode voltage. PL images taken under short circuit conditions were therefore subtracted from all images taken at other operating points in this study. It should be noted that there is an upper limit for the series resistance, beyond which this correction method will fail, because in areas of extremely high series resistance (or completely isolated regions) even an external short circuit will leave the junction at some finite voltage. We estimate that the method should work for series resistance values $<16\ \Omega\ \text{cm}^2$, which is well above the values reported in the experimental section below.

Another factor that can lead to an erroneous correlation between the luminescence signal and the diode voltage is a variation of the minority carrier lifetime within the range of 0.1–50 μs, for which the diffusion length varies between 10 and 400 μm in *p*-type silicon. Within that lifetime range the luminescence signal is essentially linear in the diffusion length for constant diode voltage.[11] Because variations of the minority carrier lifetime within that range are typical in industrial silicon solar cells (especially in multicrystalline cells) a calibration of the local PL signal $I_{\text{PL},i}$ into a local diode voltage U_i according to[12]

$$I_{\text{PL},i}=C_i\exp\left(\frac{eU_i}{kT}\right) \tag{2}$$

must be performed with individual calibration constants C_i for each position of the cell (i.e., each pixel).

Two luminescence images are therefore required for the determination of $\Delta U_{R_{s,i}}$ in order to eliminate the influence of a laterally variable minority carrier lifetime (diffusion

[a]Fax: +61-2-9662 4240. Electronic mail: thorsten@trupke.de

length) on the result, an approach that is similar to the LIT based techniques that were presented in Ref. 3. A first PL image, we call it the calibration image, is taken with low illumination intensity and under open circuit conditions. Series resistance effects in the emitter due to lateral current flow can then be assumed to be small. As a result U_i is assumed to be laterally homogeneous and equivalent to the terminal voltage U. With $U_i = U$ Eq. (2) is used to determine the local calibration constants C_i from the calibration image and the measured cell voltage.

A second PL image is taken with higher illumination intensity but at an operating point at which a large fraction of the short circuit current is extracted from the cell. The luminescence intensity $I_{\mathrm{PL},i}$ from that second measurement (corrected for the intensity from the short circuit image) is converted into a local diode voltage U_i according to Eq. (2) using the local calibration factors C_i that were determined from the calibration image. The local voltage drop over the series resistance is

$$\Delta U_{R_{s,i}} = U - \frac{kT}{e} \ln\left(\frac{I_{\mathrm{PL},i}}{C_i}\right), \tag{3}$$

with $I_{\mathrm{PL},i}$ the luminescence intensity from the second PL image. Assuming an ideal diode behavior the local current density J_i is calculated according to

$$J_i = J_{\mathrm{SC}} - J_0 \exp\frac{eU_i}{kT} = J_{\mathrm{SC}} - J_0 \frac{I_{\mathrm{PL},i}}{C_i}, \tag{4}$$

where J_0 is the total dark current density, which is calculated from the short circuit current density and the open circuit voltage of the cell and $I_{\mathrm{PL},i}$ is the luminescence intensity from the second PL image.

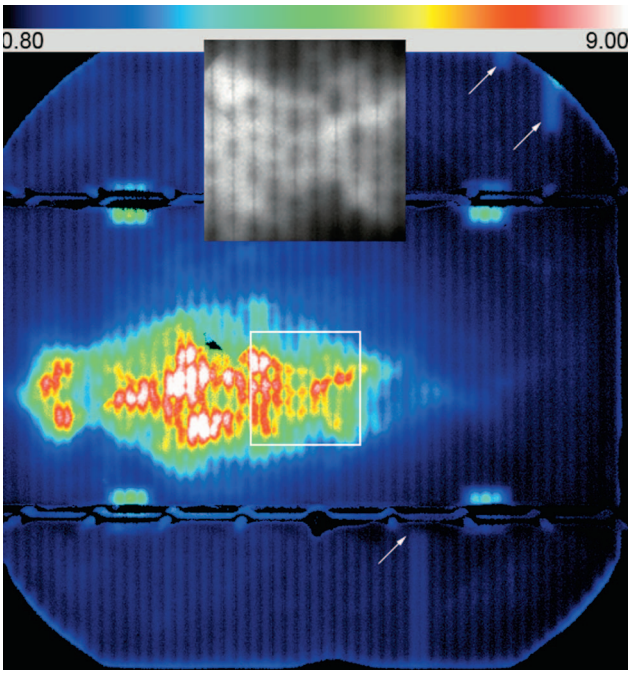

FIG. 1. (Color) Series resistance image of a screen printed monocrystalline silicon solar cell. The color bar gives the series resistance in $\Omega\,\mathrm{cm}^2$. Values of $\sim 1\ \Omega\,\mathrm{cm}^2$ in the dark areas are typical for screen printed solar cells. Very high values up to $9\ \Omega\,\mathrm{cm}^2$ in the central region are the origin of the low fill factor and efficiency of that cell. The influence of several broken grid fingers is also observed (arrows). The inset shows a grayscale closeup of the high series resistance area marked with a white frame.

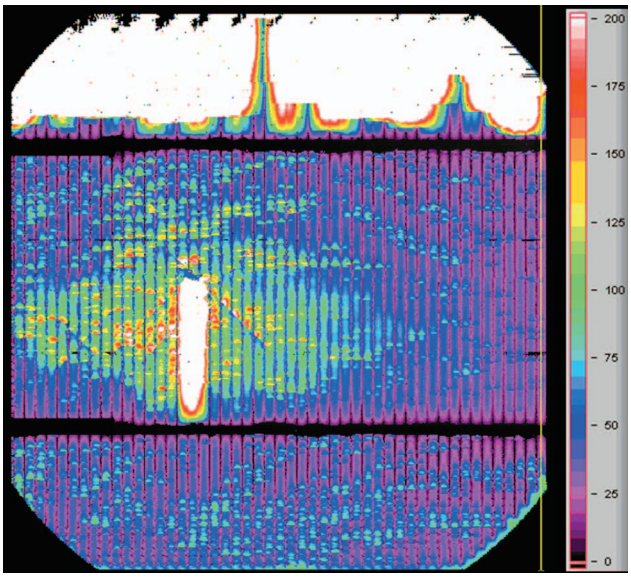

FIG. 2. (Color) Potential distribution in millivolts from a Corescan measurement taken with 10 mA cm^{-2} current density and 0.2 mm line spacing. Data acquisition time was 1 h. Some artefacts (white regions) are caused by nonoptimal hardware settings of the Corescan instrument (see text for details).

That method is demonstrated here on a monocrystalline screen printed cell, in which lateral variations of J_0 are assumed to be small. In that case using a constant J_0 for different areas of the cell is an acceptable approximation because close to short circuit conditions the expected small variations of J_0 result in even smaller lateral variations of the extracted current density J_i. While resulting in longer data acquisition times, it is thus desirable to measure the second PL image with a large fraction of the current being extracted in order to minimize the influence of J_0 variations.

In industrial multicrystalline solar cells the diffusion length can be smaller than the thickness and the bulk minority carrier lifetime can dominate J_0, which can vary by a factor of 10 or more laterally across one cell. In that case the luminescence signal is proportional to the diffusion length[11] and inversely proportional to J_0. The calibration PL image can then be used to calculate a relative J_0 distribution, which can be scaled to give the correct total J_0. Again, this procedure of eliminating local variations in the material quality from the series resistance using a separate image is similar to the procedures outlined in Ref. 3.

Figure 1 shows the series resistance image obtained on a screen printed monocrystalline cell using the method described above, assuming a constant J_0. The series resistance in units $\Omega\,\mathrm{cm}^2$ is obtained by replacing the current in Eq. (1) by the current density J_i. The calibration image was measured with 0.19 Sun equivalent illumination and under open circuit conditions (see Ref. 7, Fig. 5 for an open circuit PL image of that cell) and the second image was measured with 0.67 Sun illumination and with 81% of the photocurrent being extracted. The series resistance is dominated by a high series resistance region in the central area of the cell and by four square shaped areas underneath the busbars. The substantially enhanced series resistance in the central region limits the efficiency of that cell to 14.4% compared to 16.2% for typical cells from the same batch. Zooming into the region of enhanced series resistance (grayscale inset of Fig. 1) shows a variation of dark and bright areas along the metal grid fingers, showing in which positions the metal fingers make

good and poor contact, respectively, to the emitter, demonstrating that the series resistance is dominated by variations in the contact resistance. For comparison Fig. 2 shows the potential distribution from a Corescan measurement taken with 10 mA/cm^2 current density and 0.2 mm line spacing. The data acquisition time for that measurement was 1 h. The Corescan measurement shows good qualitative agreement with the luminescence results except for the square shaped areas under the busbars and for the extremely high series resistance (white regions) that the Corescan predicts in the area above the upper busbar of the cell and within a small area in the center. The latter series resistance features were introduced by the contact probe of the Corescan effectively isolating those regions during the measurement. Such artefacts are normally not observed in Corescan measurements and were caused here by non-ideal mechanical settings (pressure and inclination of the probe) of the instrument for this specific cell. The square shaped regions of enhanced series resistance that are observed in the luminescence image are caused by silver soldering pads on the rear surface of the cell. Because the Corescan scans the electrochemical potential at the front surface it is not sensitive to those rear contact effects.

A value of $R_{s,\mathrm{tot}}=9\ \mathrm{m}\Omega$ is calculated for the total series resistance according to

$$\frac{1}{R_{s,\mathrm{tot}}}=\sum_i \frac{1}{R_{s,i}}. \tag{5}$$

Analyzing an illuminated and a dark *IV* measurement of that cell we obtain values between $R_{s,\mathrm{tot}}=5.5\ \mathrm{m}\Omega$ at open circuit conditions increasing to $R_{s,\mathrm{tot}}=11.6\ \mathrm{m}\Omega$ at the maximum power point. These values are consistent with the total series resistance obtained from the luminescence image, given that the second PL image (with 0.67 Sun illumination and 81% current extraction) was measured slightly above the maximum power point.

This letter demonstrates a quantitative determination of the spatially resolved series resistance from two luminescence images, one open circuit PL image taken with low illumination intensity and one PL image taken with higher illumination intensity and with a large fraction of the photocurrent being extracted. For higher accuracy both images must be corrected for the diffusion limited carrier density by subtracting a PL image with the corresponding illumination intensity but taken under short circuit conditions. Because areas of high series resistance appear bright in the PL image taken with current extraction, these areas are clearly distinguished from low lifetime or shunted regions, whereas in EL images all these features appear as dark regions and are correspondingly more difficult to distinguish from each other. The smaller light intensity in the first PL image provides the calibration constant C_i under injection conditions that are comparable to the second image, thereby minimizing the potential influence of a laterally variable injection level dependence of the minority carrier lifetime.

In this study the first and the second luminescence images were taken with data acquisition times of 5 s each, resulting in a series resistance image with 125 μm spatial resolution. With 3×3 binning the same signal to noise ratio can be achieved with nine times shorter data acquisition time, allowing the total data acquisition time to be reduced to 1 s if necessary. It should also be noted that the detailed analysis described above is only required for a *quantitative* analysis of series resistance variations. A *qualitative* localization of regions of high series resistance can be accomplished in one second per cell even without binning.

The luminescence based method of determining the series resistance described here is associated with experimental errors arising predominantly from the assumptions that have to be made in calculating the local current density. While a constant J_0 was assumed in the analysis of the monocrystalline cell shown here, the local variation of J_0 must be accounted for explicitly for multicrystalline silicon solar cells. For the case studied here we estimate relative errors in the resulting series resistance values to be on the order ±20%. Similar to LIT based techniques[3] the determination of lateral series resistance variations from luminescence imaging is thus fundamentally somewhat less quantitative than Corescan or Cello measurements. On the other hand luminescence imaging has the advantage that it is nondestructive, that it is several orders of magnitude faster for comparable spatial resolution, and that it provides information about series resistance effects occurring on both the front and the rear surface.

The authors would like to thank Otwin Breitenstein for pointing out references from the literature and also Mohan Narayanan, Jessie Copper, and Angus Keenan from BP Solar for providing the cells investigated in this study and for assisting with Corescan and *IV* measurements. The Centre of Excellence for Advanced Silicon Photovoltaics and Photonics is supported under the Australian Research Council's Centres of Excellence Scheme.

[1] A. S. H. van der Heide, A. Schöenecker, G. P. Wyers, and W. C. Sinke, Proceedings of the 16th European Photovoltaic Solar Energy Conference, Glasgow, UK, 2000, p. 1438.
[2] J. Carstensen, G. Popkirov, J. Bahr, and H. Föll, Sol. Energy Mater. Sol. Cells **76**, 599 (2003).
[3] O. Breitenstein, J. P. Rakotoniaina, A. S. H. van der Heide, and J. Carstensen, Prog. Photovoltaics **13**, 645 (2005).
[4] J. Isenberg, A. S. H. van der Heide, and W. Warta, Proceedings of the 31st IEEE Photovoltaic Specialists Conference, Orlando, FL, 2005, p. 907.
[5] T. Trupke, R. A. Bardos, M. C. Schubert, and W. Warta, Appl. Phys. Lett. **89**, 044107 (2006).
[6] T. Fuyuki, H. Kondo, Y. Kaji, T. Yamazaki, Y. Takahashi, and Y. Uruoka, Proceedings of the 31st IEEE Photovoltaic Specialists Conference, Orlando, FL, 2005, p. 1343.
[7] T. Trupke, R. A. Bardos, M. D. Abbott, F. W. Chen, J. E. Cotter, and A. Lorenz, Proceedings of the 4th World Conference on Photovoltaic Energy Conversion, Waikoloa, HI, 2006, p. 928.
[8] M. Kasemann, M. C. Schubert, M. The, M. Köber, M. Hermle, and W. Warta, Appl. Phys. Lett. **89**, 224102 (2006).
[9] K. Schick, E. Daub, S. Finkbeiner, and P. Würfel, Appl. Phys. A: Solids Surf. **A54**, 109 (1992).
[10] T. Trupke, R. A. Bardos, M. D. Abbott, and J. E. Cotter, Appl. Phys. Lett. **87**, 093503 (2005).
[11] T. Fuyuki, H. Kondo, T. Yamazaki, Y. Takahashi, and Y. Uraoka, Appl. Phys. Lett. **86**, 262108 (2005).
[12] P. Würfel, *Physics of Solar Cells* (Wiley-VCH, Weinheim, 2005), Vol. 1, p. 139.